2014 International Joint Conference on Neural Networks (IJCNN)
July 6-11, 2014, Beijing, China

Application of fuzzy systems in the control of a shunt active power filter with four-leg topology

Edson J. Acordi, Ivan N. da Silva, Ricardo Q. Machado

Abstract—**This paper presents the application of fuzzy controllers to act in the current control loop of a shunt active power filter (SAPF). The SAPF consists of a three-phase inverter with four-leg topology, and it has been used to reduce the harmonic content produced by nonlinear loads, as well as, in the reactive power compensation. The generation of the reference currents is based on the synchronous reference frame (SRF), which requires the use of a PLL (Phase Locked Loop) synchronization algorithm with the grid. The classic PI control is here replaced by a fuzzy controller that has features that allows fast convergence and robustness when there are parametric variations in the physical system. Results obtained from simulations are presented to validate the approach and to demonstrate the performance of the filter in the suppression of harmonic currents and reactive power.**

I. INTRODUCTION

CURRENTLY, with the development of power electronics and consequently the proliferation of nonlinear loads connected to the electrical system, many problems related to power quality (PQ) have arisen. These loads are formed mainly by static power converters, and because of their nonlinear characteristics, they drain currents from the mains with high level of harmonic distortion, which may cause deformations on the grid voltage. Among the problems caused by the deformation of the input currents, it is possible to mention the voltage distortion at the point of common coupling (PCC), that occurs due to the interaction of the harmonic currents with the impedance of the utility grid, which may result in malfunction of the equipment connected to the same PCC [1]-[3]. Furthermore, it can be observed transformers overheating, reduction of the power factor and increasing of the current drawn by electric motors. One of the most common methods for filtering harmonic currents and compensate the reactive power is through the shunt passive power filters (SPPF). However, the SPPF can resonate with the power supply when the impedance of the system changes, which may result in damage in the equipment connected to the mains [4]-[6]. Thus, the shunt active power filters (SAPF) are an alternative to the problems and limitations presented by SPPF. They have high output impedance, which implies in the reduction of the resonance occurrence. In addition, they are less bulky and adjust themselves dynamically with the harmonics present in the loads [7]. Within this context, the power electronics plays an important role to ensure the efficient processing of energy [8]. The operating principle of SAPF is illustrated in Fig. 1. The SAPF acts injecting/absorbing current at the grid connection point, making the current absorbed from the network ideally sinusoidal, thereby, the network provides only the fundamental waveform whereas the SAPF, the harmonic portion.

To the SAPF operate properly, the strategy used in the generation of the compensation currents have to be able to separate accurately the fundamental term of the load current from the harmonic components.

Furthermore, the technique used for the control should be able to do the filter impose correctly the compensation currents. Another additional feature of the SAPF is the capability to perform reactive power compensation of with minimal modifications in the strategies that produces the reference currents [8].

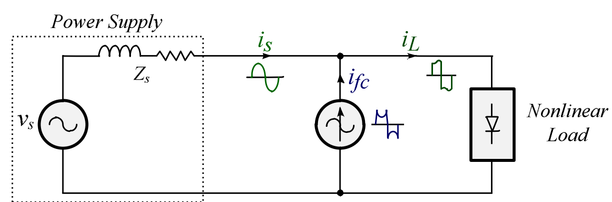

Fig. 1. Operating principle of SAPF.

The SRF based algorithm was used as technique for extract the reference currents [6], [9]. Among the main inverter topologies that allow the control of the neutral current the Split-Capacitor, Three-Full Bridge and Four-Legs are the most useful structures. A detailed study of the mathematical models involving the Four-Legs and Three-Full Bridge topologies is shown in [10].

The control techniques applied in SAPF typically use PI or PID controllers, which are adjusted taking into account the linear model of the physical system. Although their design is simple, with satisfactory results, they may present steady-state error [11]. Thus, fuzzy logic controllers have been proposed as an alternative to the limitations imposed by classical controllers [12]-[14].

This work proposes the use of fuzzy controllers in the current control loop of the SAPF in order to obtain features that are not presented in classical PI controller, for example, low rejection of disturbances, nonlinear control, and therefore being a more robust controller [15].

Edson. J. Acordi is with the Instituto Federal do Paraná (IFPR), PR466 - Gleba Pindaúva Secção C, Parte 2 – Ivaiporã PR, Brazil. (e-mail: edson.acordi@ifpr.edu.br).

Ivan. N. da Silvar is with Departamento de Engenharia Elétrica, Universidade de São Paulo (USP). Av. Trabalhador Sancarlense, 400 – centro, São Carlos SP, Brazil. (e-mail: insilva@sc.usp.br).

Ricardo Q. Machado is with Departamento de Engenharia Elétrica, Universidade de São Paulo (USP). Av. Trabalhador Sancarlense, 400 – centro, São Carlos SP, Brazil. (e-mail: rquadros@sc.usp.br).

The authors gratefully acknowledge the contributions of the FAPESP (Process 2011/17610-0) by the financial support for the development of this research.

To validate the proposed control methodology, results of computer simulations are presented to evaluate the performance of SAPF in the ability to suppress the harmonic currents.

II. System Description

A. Four-legs SAPF

The topology of four-leg inverter used is shown in Fig. 2. This kind of structure uses 8 insulated-gate bipolar transistor (IGBT) allowing full compensation of current flowing through the neutral conductor without presenting problems of dynamic response as has been reported in the inverter-Split Capacitor, besides of the fact that it can work with a 15% smaller value of the DC-link voltage [16]. Thus, this topology is better suited for applications where it is desired to compensate the zero-sequence current, although it requires a larger number of IGBT [17]. As the four-leg topology, the Three-Full Bridge also allows complete compensation of the neutral current without any reduction in performance of the filter however 12 IGBTs are required.

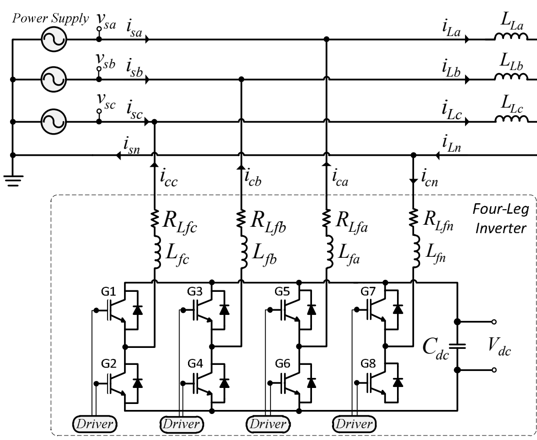

Fig. 2. Four-leg inverter topology.

B. Reference currents and control strategy

To generate the reference currents, the method based on SRF is applied, where the load currents (i_{La}, i_{Lb}, i_{Lc}) are measured and transformed from (*abc*) to (*αβ*) by means of the Park transformation. Thereby, the two-phase stationary system in (*αβ*) is given as shown in (1).

$$\begin{bmatrix} i_\alpha \\ i_\beta \\ i_0 \end{bmatrix} = \sqrt{\frac{2}{3}} \begin{bmatrix} 1 & -\frac{1}{2} & -\frac{1}{2} \\ 0 & \frac{\sqrt{3}}{2} & -\frac{\sqrt{3}}{2} \\ \frac{1}{\sqrt{2}} & \frac{1}{\sqrt{2}} & \frac{1}{\sqrt{2}} \end{bmatrix} . \begin{bmatrix} i_a \\ i_b \\ i_c \end{bmatrix} \tag{1}$$

In sequence, the *αβ* currents are transformed to the synchronous reference system (*dq*), through (2), where *sin(θ)* and *cos(θ)* are the unit vectors obtained from the PLL (Phase-Locked Loop) [18] in grid-tie operation.

$$\begin{bmatrix} id \\ iq \end{bmatrix} = \begin{bmatrix} cos(\theta) & sin(\theta) \\ -sin(\theta) & cos(\theta) \end{bmatrix} . \begin{bmatrix} i_\alpha \\ i_\beta \end{bmatrix} \tag{2}$$

Therefore, the currents in synchronous reference frame (*dq*) are composed by the dc and ac parts. The dc part represents the fundamental terms (active and reactive) of the load currents and the ac portion represents the harmonic components, which can be extracted through the use of a high-pass filter (HPF). The block diagram of the SRF based algorithm is shown in Fig. 3.

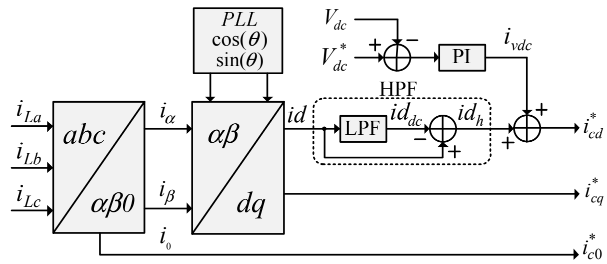

Fig. 3. Block diagram of SRF based algorithm.

The direct-axis current (id) is the sum of active fundamental current (id_{dc}) with the harmonic portion of the load current (id_h) according to (3).

$$id = id_{dc} + id_h \tag{3}$$

Applying a low-pass filter (LPF) on the id current, id_{cc} is obtained, which it represents the fundamental active current in the synchronous d-axis. Additionally, the ac which is the harmonic component is obtained by subtracting the total id current from the id_{cc} part. In this way, the result is characterized as the harmonic portion of the load current. The quadrature-axis current (iq) is the sum of the fundamental reactive portion (iq_{cc}) with the harmonic reactive parcel (iq_h). The iq current is not filtered as shown in Fig. 3, thus, besides the harmonic reactive compensation, is also possible the compensation of the reactive portion of the fundamental load current. Furthermore, the whole i_0 current is used to produce the reference current through the neutral to obtain a balanced power flow between the grid and load. Thus, the phase currents are balanced and the neutral current equal to zero. For the DC-link voltage, a PI controller is used to provide an additional amount of active current (i_{vdc}) and promote the its balancing, which is added in direct-axis reference current (id).

The reference compensation currents ($i_{cd}^*, i_{cq}^*, i_{c0}^*$) shown in Fig. 3, are then compared with the currents imposed by SAPF (i_{cd}, i_{cq}, i_{c0}) and then employed as inputs (e_d, e_q, e_0) into the fuzzy controllers (Fig. 4). Then, they are again transformed to the αβ axes through the equation (4).

$$\begin{bmatrix} v_{c\alpha}^* \\ v_{c\beta}^* \\ v_{c0}^* \end{bmatrix} = \begin{bmatrix} \cos(\theta) & -sin(\theta) & 0 \\ sin(\theta) & \cos(\theta) & 0 \\ 0 & 0 & 1 \end{bmatrix} . \begin{bmatrix} v_{cd}^* \\ v_{cq}^* \\ v_{c0}^* \end{bmatrix} \tag{4}$$

Where, v_{cd}^*, v_{cq}^* and v_{c0}^* are the respective outputs of fuzzy controllers in *dq0* coordinates, considering the uncoupling of the current of direct and quadrature axes [10].

The control actions $v_{c\alpha}^*$, $v_{c\beta}^*$ and v_{c0}^* are then taken to the space vector modulation (SVM) [19], [20] which will cause activation of the IGBTs in order to correctly synthesize the compensation currents.

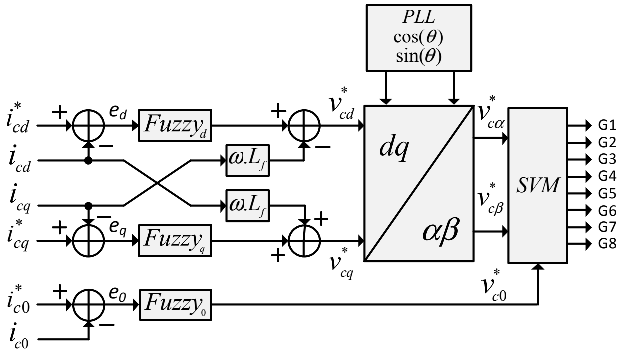

Fig. 4. Fuzzy controllers.

Note in Fig. 4, that for determination of the error signal led to the inputs fuzzy controllers, and for decoupling the currents of direct and quadrature axis, it is necessary to calculate the currents imposed by the filter in coordinates $dq0$ (i_{cd}, i_{cq}, i_{c0}). This is accomplished as shown in Fig. 5.

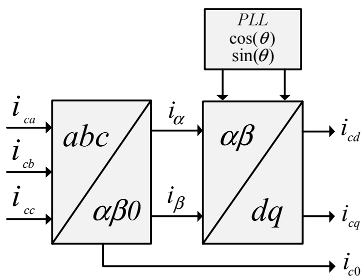

Fig. 5. Currents imposed by SAPF.

III. Fuzzy Controllers of Current Loops

The theory of fuzzy sets are based on the studies proposed by Zadeh in 1965 [21], where the concepts were used to describe systems with imprecise information about a particular process through sets of linguistic rules. The fuzzy controllers are based on the knowledge of the process, where it is possible to synthesize the functioning of a system through the control routines that allow the particularities of the system to be maintained. Thus, an inference system grounded in applied rules based on set theory and fuzzy logic consist of mathematical tools for the implementation of control systems with linguistic rules. Initially, for the accomplishment of fuzzy design controller, the information are collected from the process described by an expert, where they are parameterized in order to obtain a satisfactory controller. The fuzzy controllers are basically composed of 4 main components, fuzzification system, inference, defuzzification system and database/rules [22]. For the strategy adopted in this paper, three fuzzy controllers are needed, in axes d, q and 0, respectively. The controllers of the dq axes have the same adjustment, since the models that represent the physical system are similar. However, for the controller in the 0 axis, the adjustment of fuzzy rules is different due to the model associated with this axis [10], [20].

Figure 6 shows the block diagram of the implemented fuzzy controllers.

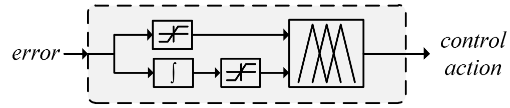

Fig. 6. Block diagram of the fuzzy controllers.

The fuzzy controller has two inputs, one with the signal of the error and the other with the integral of error and a single output, which is the signal of the control action. The membership function of the input signals were defined according to Fig. 7.

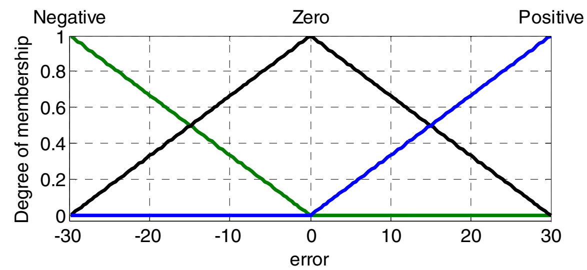

Fig. 7. Membership function of input signal (*error*).

On the other hand, the membership function of the integral part of the dq axes were defined as shown in Fig. 8.

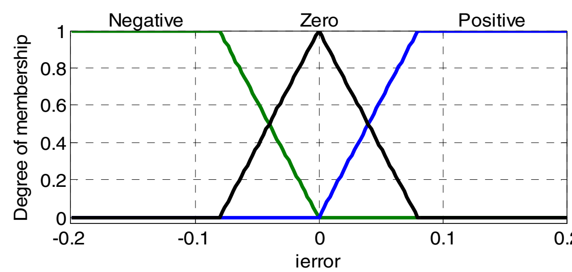

Fig. 8. Membership function of the integral input signal (dq axes).

Whereas, the adjustment of the membership function of the output signal in dq axes, were defined as shown in Fig. 9.

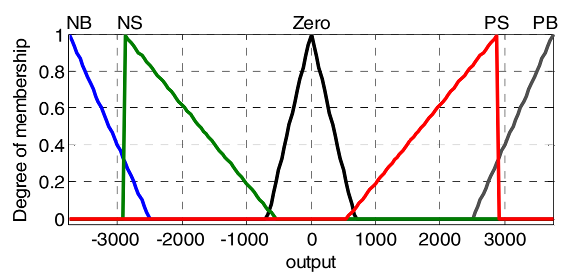

Fig. 9. Membership function of the output signal (dq axes).

Note that, NB and NS represent the numerical variables into linguistic variables; negative big and negative small respectively. Similarly, PS and PB are positive small and positive big. The membership function of the integral part of the input signal for the zero axis controller is parameterized as shown in the Fig. 10.

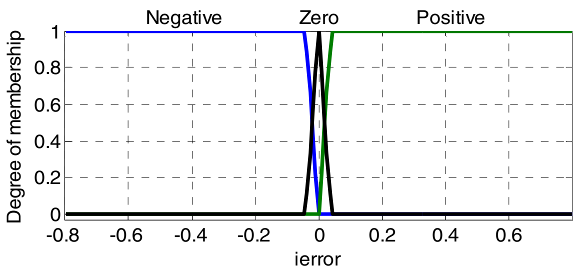

Fig. 10. Membership function of the integral input signal (0 axis).

For setting the membership function of the output signal for the 0-axis controller, the adjustment was made as seen in Fig. 11.

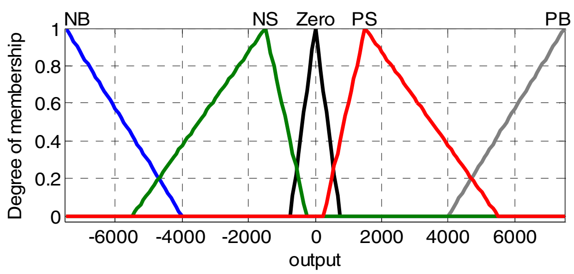

Fig. 11. Membership function of the output signal (0 axis).

In fuzzy controllers, the implication operator of type MIN was used and for the defuzzification, the centroid method (central-of-areas) was applied.

In the implementation of fuzzy controllers, nine implication rules were defined, as shown in the Table I, where the *error* represents the input signal and *ierror* the integral of the input signal, and *act* the output signal (control action).

TABLE I
IMPLICATION RULES OF FUZZY CONTROLLERS

Rules	Condition	Action
1	If (*error*<0) and (*ierror*<0)	*act* = NB
2	If (*error*<0) and (*ierror*=0)	*act* = NB
3	If (*error*<0) and (*ierror*>0)	*act* = NB
4	If (*error*=0) and (*ierror*<0)	*act* = NS
5	If (*error*=0) and (*ierror*=0)	*act* = Zero
6	If (*error*=0) and (*ierror*>0)	*act* = PS
7	If (*error*>0) and (*ierror*<0)	*act* = PB
8	If (*error*>0) and (*ierror*=0)	*act* = PB
9	If (*error*>0) and (*ierror*>0)	*act* = PB

Figure 12 shows the control surface of axes *dq* and *0*. Note that the control surface is not linear, unlike PI controllers. The control surface is represented declaratively on database and executed by rules defined to the controller.

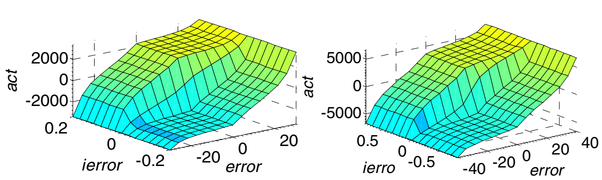

(a) (b)

Fig. 12. Fuzzy control surface. (a) *dq* axes; (b) *0* axis.

IV. SIMULATION RESULTS

This section presents the results of simulations with Matlab/Simulink software to the SAPF with fuzzy controllers applied in the current loops in replacement of the traditional PI. The simplified topology of the simulated system is shown in Fig. 13, which is formed by the power supply, load and the SAPF connected in parallel with the load.

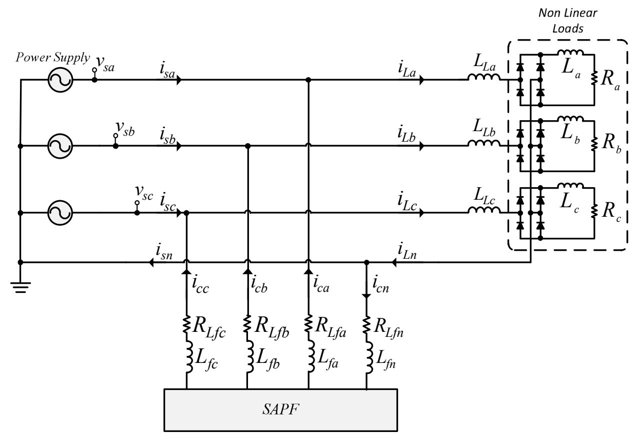

Fig. 13. Simplified schematic of the simulated system.

The parameters used in the simulations are shown in Table II. The simulation was entirely discretized, so that the values stay as close as possible to a real system.

TABLE II
PARAMETERS OF THE SIMULATED SYSTEM

Supply Voltage (V_{rms})	127 V
Supply frequency (*f*)	60 Hz
Filtering Inductance (L_f)	1 mH
AC Inductance (L_l)	1.2 mH
Series resistance of the Filtering Inductance (R_{Lf})	0.20 Ω
DC bus voltage (V_{dc})	400 V
DC Bus capacitance (C_{dc})	4.7 mF
Sampling frequency (f_s)	40 kHz
Switching frequency (f_{sw})	20kHz

The parameters of the loads are shown in Table III. The load 1 consists of three rectifiers single-phase full-wave with elements RL (Resistive-Inductive) in series. The load 2 has the same rectifier configuration but with elements RC (Resistive-Capacitive) in parallel in rectifier of phase 'c'.

TABLE III
LOAD PARAMETERS

	Phase 'a'	Phase 'b'	Phase 'c'
Load 1	R_a=4.8 Ω L_a=13 mH	R_b=5.9 Ω L_b=18 mH	R_c=8.8 Ω L_c=22 mH
Load 2	R_a=4.8 Ω L_a=13 mH	R_b=5.9 Ω L_b=18 mH	R_c=25 Ω C_c=940 μF

The currents waveforms of the simulated system considering the load 1 are shown in Fig. 14. The load currents i_{La}, i_{Lb}, i_{Lc} and i_{Ln} are shown in Fig. 14 (a), where it is possible to note that these are unbalanced and have non-sinusoidal characteristics. The Fig. 14 (b) shows the phase currents drained from the mains (i_{sa} , i_{sb} , i_{sc} and i_{sn}) after compensation held by SAPF, where it can be observed that they became practically sinusoidal and balanced, and the neutral current (i_{sn}) is very close to zero, as expected.

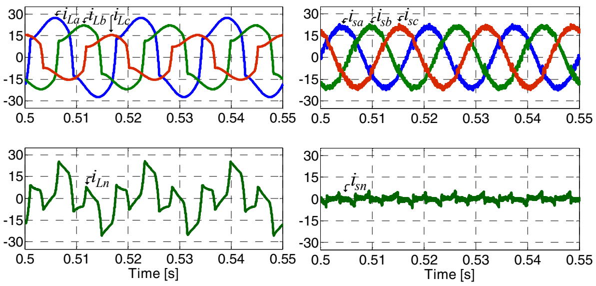

(a) (b)

Fig. 14. Currents of the system. (a) Load currents i_{La}, i_{Lb}, i_{Lc} and i_{Ln}; (b) Mains currents i_{sa}, i_{sb}, i_{sc} and i_{sn}.

For load 2, the results are shown in Fig. 15 (a) and (b) respectively. Note that the rectifier current of the phase 'c', has a higher harmonic content than the other phases because of the RC elements. Even in this situation, the fuzzy controllers designed were able to do the SAPF impose adequately the compensation currents, since the currents drained from the grid were practically sinusoidal and balanced resulting in a neutral current (i_{sn}) very close to zero. It is observed that the compensated current of phase 'c' was slightly more distorted compared with the load 1 because there is a greater effort of the SAPF to follow the high rates of current changing presented by the rectifier with RC elements.

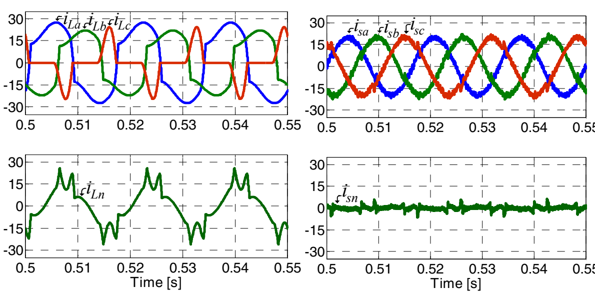

(a) (b)

Fig. 15. Currents of the system. (a) Load currents i_{La}, i_{Lb}, i_{Lc} and i_{Ln}; (b) Mains currents i_{sa}, i_{sb}, i_{sc} and i_{sn}.

The total harmonic distortions of the source currents before and after the compensation of the SAPF with fuzzy/PI controllers are presented in Table IV. Note that the harmonic content of the source currents were reduced from the 22-24% to approximately 5-6%. For the load 2, that represents the worst case, the phase 'c' had a reduction from 83.9% to 7.65%, showing the effectiveness of the fuzzy controllers.

TABLE IV
TOTAL HARMONIC DISTORTION OF THE CURRENTS

	THD (%)								
	Load Currents			SAPF with Fuzzy Controllers			SAPF with PI Controllers		
	Phases			Phases			Phases		
Load	'a'	'b'	'c'	'a'	'b'	'c'	'a'	'b'	'c'
1	22.1	24.8	24.03	5.24	6.02	5.37	5.17	5.77	4.98
2	22.3	25.1	83.90	6.15	6.05	7.65	5.93	6.08	7.51

As shown in Table IV, the results obtained with the PI and fuzzy controllers are very similar. Another simulation was performed to evaluate the results of the SAPF under conditions of parametric variation of the physical system, both for the fuzzy controller as for PI. In this case were considered that supply voltage has a 5.08% of THD, with filtering inductance $L_f = 0.8mH$. Furthermore, a step load of 50% was added at time 0.5s. The results are shown in Fig. 16 (a) and (b).

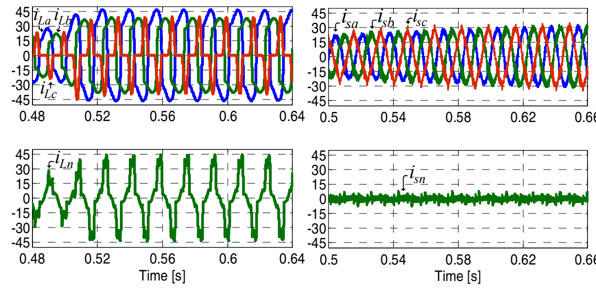

(b) (b)

Fig. 16. Currents of the system. (a) Load currents i_{La}, i_{Lb}, i_{Lc} and i_{Ln}; (b) Mains currents i_{sa}, i_{sb}, i_{sc} and i_{sn}.

In this case, the total harmonic distortions of the source currents are presented in Table V. Note that the fuzzy controllers showed better performance than the PI. For fuzzy controllers, the THD has reduced to approximately 11-12%, while PI decreased to 15-17%.

TABLE V
TOTAL HARMONIC DISTORTION OF THE CURRENTS

	THD (%)								
	Load Currents			SAPF with Fuzzy Controllers			SAPF with PI Controllers		
	Phases			Phases			Phases		
Load	'a'	'b'	'c'	'a'	'b'	'c'	'a'	'b'	'c'
1	26.4	28.7	30.10	11.37	12.44	12.52	15.24	15.17	17.18
2	27.6	29.8	67.90	12.17	12.77	11.19	17.14	16.47	17.86

For all simulations, the THD was evaluated up to the 51st harmonic, and 10 cycles of the current were considered.

V. CONCLUSION

This work presented the application of fuzzy systems to control the current loop of the SAPF with four-leg topology. The principle of operation of the SAPF was presented, as well as the technique for generating the reference currents and the applied algorithm, which is based on the synchronous reference frame (SRF). The control of the SAPF was performed in the *dq0* synchronous coordinated system using three fuzzy controllers responsible for ensuring that the compensation currents of SAPF are imposed properly on the mains. Through the simulations, it was observed that the fuzzy controllers have provided an appropriate operation of the SAPF in suppression of the harmonics of load current and reactive power compensation, so that the currents absorbed from the grid become approximately sinusoidal and balanced, thus providing improvement of the power quality in the presence of nonlinear loads.

ACKNOWLEDGMENT

The authors gratefully acknowledge the contributions of the FAPESP (Process 2011/17610-0) by the financial support for the development of this research.

REFERENCES

[1] M. Singh, & A. Chandra, "Real Time Implementation of ANFIS Control for Renewable Interfacing Inverter in 3P4W Distribution Network," IEEE Trans. Industrial Electronics, vol. 1, Jan. 2013.

[2] R. M. Potdar, "Comparison of Topologies of Shunt Active Power Filter Implemented on Three Phase Four-Wire System," International Journal of Soft Computing and Engineering (IJSCE), vol. 1, no. 5, pp. 209-216, Nov. 2011.

[3] H. Akagi, "New trends in active filters for power conditioning," IEEE Transactions on Industry Applications, vol. 32, pp. 1312-1322, Nov./Dec. 1996.

[4] H. Akagi, Y. Kanagawa, A. Nabae, "Instantaneous Reactive Power Compensators Comprising Switching Devices without Energy Storage Components," IEEE Trans. Industry Applications, vol. 20, pp. 625-630, May/June 1984.

[5] B. Singh, K. AL-Haddad, and A. Chandra, "A review of active filters for power quality improvement," IEEE Transactions on Industrial Electronics, vol. 46, no. 5, pp. 960-971, Oct. 1999.

[6] D. M. Divan, S. Bhattacharya, and B. Banerjee, "Synchronous frame harmonic isolator using active series filter," in Proc. European Power Electronics Conference (EPE), pp. 30-35, 1991.

[7] Dugan, Roger C. Mcgranaghan, Mark F. Santoso, Surya. Beaty, H. Wayne, "Electrical power systems quality," 2nd ed. New York: McGraw-Hill, 2004, pp. 263.

[8] I. I. Abdalla, K. S. R Rao, N. Perumal, "A comparative study of shunt active power filter performance in distribution systems," in International Power Engineering and Optimization Conference (PEOCO2011), pp. 273-278, June 2011.

[9] S. A. O. Silva and R. A. Modesto, "A comparative analysis of SRF-based controllers applied to active power line conditioners," Proc. 34th Annual Conference of the IEEE Industrial Electronics Society (IECON2008), pp. 405-410, Nov. 2008.

[10] E. J. Acordi, L. B. G. Campanhol, S. A. O. Silva, C. B. Nascimento, A. Goedtel, "A study of shunt active power filters applied to three-phase four-wire systems," Renewable Energy & Power Quality Journal (RE&PQJ), vol. 10, p.277-279, April 2012.

[11] J. Chen, Xinjian Jiang, Dongqi Zhu, Likuan Deng, Beige Yang, "High power hybrid active power filter for medium-voltage distribution network," Electrical Machines and Systems (ICEMS), vol. 2m pp. 1381-1386, Sept. 2005.

[12] N. Gupta, S.P. Singh, S.P Dubey, "Fuzzy logic controlled shunt active power filter for reactive power compensation and harmonic elimination," 2nd International Conference on Computer and Communication Technology (ICCCT), pp. 82-87, Sept. 2011.

[13] O. Montiel, J. Olivas, R. Sepulveda, O. Castillo, "Development of an embedded simple tuned fuzzy controller," IEEE World Congress on computational Intelligence (WCCI), pp. 555-561, June 2008.

[14] S.M. Ayob, Z. Salam and N. A. Azli, "A discrete single input PI fuzzy controller for inverter applications," 33rd Annual Conference of the IEEE Industrial Electronics Society (IECON 2007), pp. 2032–2037, Nov. 2007.

[15] G. Tsengenes, A. Georgios, "Shunt active power filter control using fuzzy logic controllers," IEEE International Symposium on Industrial Electronics (ISIE), pp. 365-371, June 2011.

[16] C. A. Quinn, N. Mohan, "Active filtering of harmonic currents in three-phase, four-wire systems with three-phase and single-phase non-linear loads," Proc. Applied Power Electronics and Exposition (APEC), pp. 829-836, Feb. 1992.

[17] N. Mendalek, "Modeling and control of three-phase four-leg split-capacitor shunt active power filter," in Advances in Computational Tools for Engineering Applications (ACTEA), pp. 121-126, July 2009.

[18] L. G. B. Rolim, D. R. da Costa, M. Aredes, "Analysis and software implementation of a robust synchronizing PLL circuit based on the pq theory," IEEE Transactions on Industrial Electronics, vol. 53, no. 6, pp. 1919-1926, Dec. 2006.

[19] H. Pinheiro, et al., "Space vector modulation for voltage-source inverters: a unified approach," Proceedings of the IEEE 28th Annual Conference of the Industrial Electronics Society, IECON, pp. 23-29, Nov. 2002.

[20] E. J. Acordi, "Estudo e implementação de um filtro ativo de potência paralelo aplicado em sistemas trifásicos a quatro fios com controle e modulação vetorial", Master Thesis, Federal Technological University of Paraná (UTFPR-CP), Cornélio Procópio, Brazil, 2012. (in Portuguese)

[21] L. A. Zadeh, "Fuzzy Sets," Information and Control, vol. 8, pp. 338-353, 1965.

[22] C. C. Lee, "Fuzzy logic in control systems: fuzzy logic controller – part I," IEEE Transactions on Systems, Man and Cybernetics, vol. 20, no. 2, pp. 404-418, Mar./Apr. 1990.